JOURNAL OF APPLIED ELECTROCHEMISTRY 25 (1995) 1133–1138

Physicochemical and electrocatalytic properties of $LaNiO_3$ prepared by a low-temperature route for anode application in alkaline water electrolysis

R. N. SINGH*, A. N. JAIN, S. K. TIWARI, G. POILLERAT‡, P. CHARTIER‡

Electrochemical Laboratory, Department of Chemistry, Faculty of Science, Banaras Hindu University, Varanasi 221 005, India

Received 7 January 1995; revised 24 March 1995

$LaNi_{1-x}Fe_xO_3$ ($x = 0$, 0.25, 0.5) has been synthesized by the hydroxide solid solution precursor method for electrochemical characterization as oxygen anode in strongly alkaline medium. Studies were made at the oxide film, which was obtained by the oxide-slurry painting technique. The cyclic voltammetric study showed the formation of a diffusion-controlled quasireversible redox couple, Ni(II)/Ni(III), ($E^0 \sim 430 \pm 10$ mV) at the oxide surface in 1 M KOH. The reaction was observed to follow approximately first-order kinetics in OH^- concentration. Values of the Tafel slope ranged between 59 and 86 mV decade^{-1} with all the oxide film electrodes. The electrocatalytic activity was found to be greatest with the $Ni/LaNi_{0.75}Fe_{0.25}O_3$ electrode. A comparison was made between the electrocatalytic activities of $LaNiO_3$ prepared by the hydroxide solid solution precursor and by the hydroxide coprecipitation technique.

1. Introduction

$LaNiO_3$, prepared by the hydroxide coprecipitation technique has been reported as one of the best anodes for oxygen evolution [1], nickel in the oxide lattice being essentially in +2 oxidation state. Recently Vidyasagar *et al.* [2] synthesized this oxide by a new method, the hydroxide solid solution precursor. This method required a relatively low preparation temperature and produced nickel in the +3 oxidation state in the oxide lattice. Although the latter oxide seems to be interesting, it has not yet been studied for electrocatalysis of the oxygen evolution/reduction reaction. The change in the oxidation state of nickel in the oxide lattice might influence the electrochemical and interfacial properties of the catalyst/solution interface. Also, the modified preparation procedure may affect the properties of the oxide [3]. The oxide was prepared by the new method and investigated for physicochemical and electrocatalytic properties in relation to oxygen evolution in KOH solution. The oxide electrodes used were in the form of films on nickel supports. For comparison, $LaNiO_3$ was also prepared by the hydroxide coprecipitation technique.

2. Experimental details

$LaNi_{1-x}Fe_xO_3$ ($x = 0$, 0.25, 0.5) was prepared following the procedure of Vidyasagar *et al.* (method I) [2]. In this method, an aqueous solution containing metal nitrates in stoichiometric quantities was added to a Cl_2-saturated ~ 6 M NaOH. To ensure complete oxidation of metal ions ($Ni^{2+} \longrightarrow Ni^{3+}$), Cl_2 was passed for about 30 min after the addition of metal nitrates solution. The precipitated complex metal hydroxide was filtered, repeatedly washed with hot distilled water, dried at 100 °C and finally decomposed at suitable temperatures to obtain nickelates. $LaNiO_3$ was also prepared by the hydroxide coprecipitation method of Otagawa and Bockris (method II) [1]. The formation of Perovskite phase was confirmed by X-ray diffraction (XRD) using CoK_α radiation.

The oxide electrode was prepared in the form of a film by painting a slurry containing the oxide and Triton X-100 onto one side of the nickel support. This support was previously exposed to conc HCl for 20 min, washed with distilled water and dried in air. After painting the slurry, the plate was annealed at 400 °C for 1 h in air.

For electrochemical studies, the electrical contact with the oxide film was made as described earlier [4, 5]. Only 0.5 cm^2 area of the catalytic film was used for the study.

The electrochemical cell, reference (Hg/HgO/1 M KOH) and counter (bright Pt) electrodes used were the same as described in [6]. For studies carried out in 30 wt % KOH, the reference electrode and the cell contained the same solution. The instrumentation (bipotentiostat, electrochemical impedance system) used and the procedure followed in the determination of cyclic voltammetry, electrochemically active area, and anodic Tafel polarization were as previously

*Author to whom correspondence should be addressed.
‡Laboratoire d'Electrochimie et de Chimie–Physique du Corps Solide, URA au CNRS no. 405, Université Louis Pasteur, 4, rue Blaise Pascal, 67000 Strasbourg, France.

0021-891X

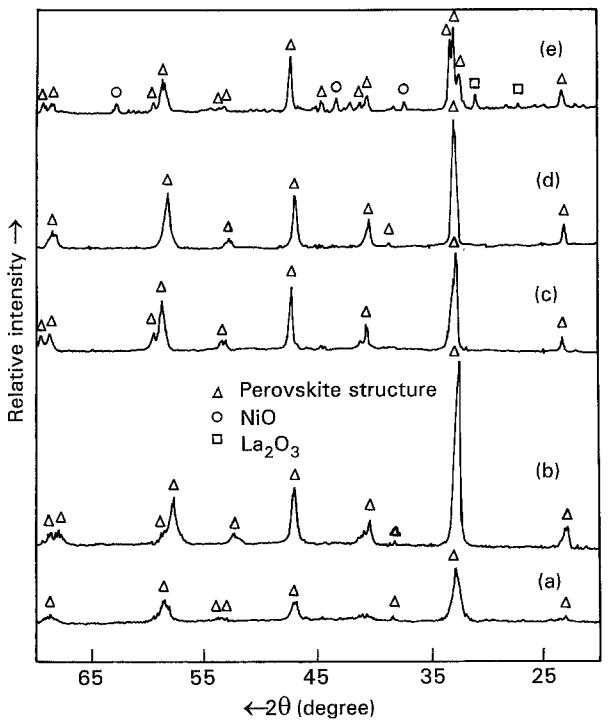

Fig. 1. XRD patterns of $LaNiO_3$ (a) 550, (b) 600, (c) 700 °C and $LaNi_{0.5}Fe_{0.5}O_3$ (d) 600 °C prepared by method I and of $LaNiO_3$ (e) 800 °C prepared by method II.

described [4]. As mentioned earlier [4] the resistance of the oxide, electrode including the solution resistance, was estimated from impedance measurements. Samples of $LaNiO_3$, prepared by the two different methods, were analysed for Ni^{3+} content iodometrically [7]. Results showed the presence of 83% Ni^{3+} in $LaNiO_3$, prepared by method I and 48% as prepared by method II.

3. Results and discussion

3.1. *X-ray diffraction studies*

Figure 1 shows the XRD patterns of $LaNiO_3$ prepared at 550 (a), 600 (b) and 700 °C (c) and $LaNi_{0.75}Fe_{0.25}O_3$ at 600 °C (d) by method I, and of $LaNiO_3$ by method II at 800 °C (e). This figure shows that the new method yields a single phase Perovskite-type oxide even at temperature as low as 550 °C. In contrast, the hydroxide coprecipitation method gives Perovskite oxide along with NiO and La_2O_3 impurities. However, under similar experimental conditions, a pure Perovskite phase was obtained by Otagawa and Bockris [1].

3.2. *Morphology of the oxide film*

The scanning electron micrographs (Fig. 2) of the catalytic films show that the method used in the oxide preparation strongly influences the morphology of the film. In the case of $LaNiO_3$ film prepared by method II, the surface is crystalline (Fig. 2(a)) and the crystallites adopt a more or less spherical shape. This morphology was not found in the $LaNiO_3$ film

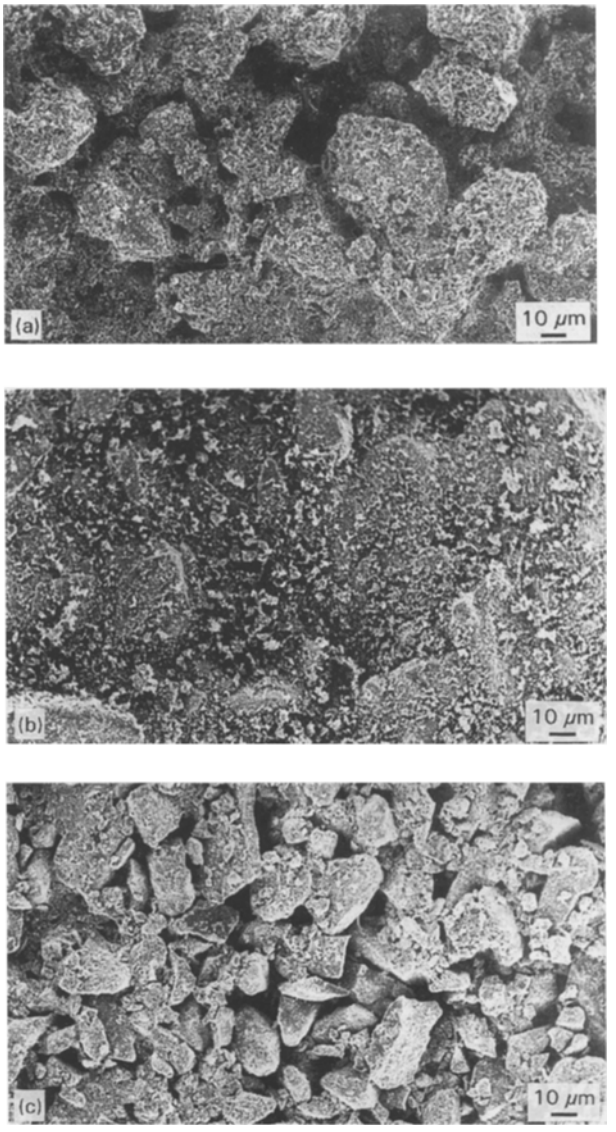

Fig. 2. SEM micrographs: (a) $LaNiO_3$ prepared by method II, (b) $LaNiO_3$ prepared by method I and (c) $LaNi_{0.75}Fe_{0.25}O_3$ prepared by method I.

obtained by method I (Fig. 2(b)). In this case grains are comparatively small and are in a highly dispersed form; however, 0.25 mole iron substitution for nickel in the oxide lattice (Fig. 2(c)) enhances the grain size and the surface again appears crystalline.

3.3. *Cyclic voltammetry*

Typical cyclic voltammograms at 20 $mV\,s^{-1}$ in 1 M KOH for $LaNiO_3$ (A) and $LaNiO_{0.75}Fe_{0.25}O_3$ (B) prepared by method I and $LaNiO_3$ (C) prepared by method II are shown in Fig. 3. These voltammograms are similar in nature and show a single anodic and a corresponding cathodic peak before the onset of oxygen evolution.

The effect of oxide loading in the case of electrode A was also investigated. It was noted that the position of the cathodic peak remained practically unchanged, regardless of the oxide loading but the anodic peaks gradually shifted in the anodic direction with increasing oxide loading. Voltammetric analysis showed that

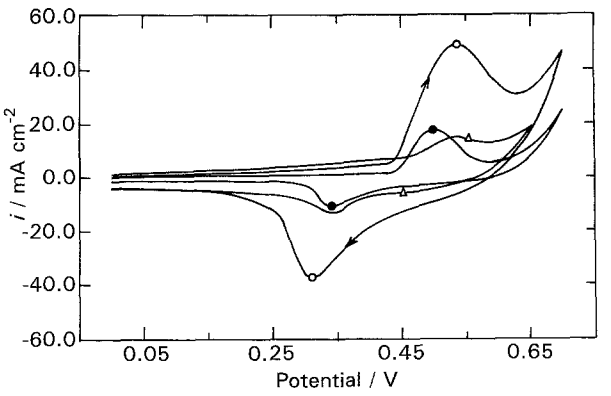

Fig. 3. Cyclic voltammograms of lanthanum nicklate films on nickel at a potential scan rate of $20\,mV\,s^{-1}$ in 1 M KOH at 25 °C; (○) $LaNiO_3$ and (△) $LaNi_{0.75}Fe_{0.25}O_3$ (method I) and (●) $LaNiO_3$ (method II).

the increase in oxide loading from 4.36 to $25.4\,mg\,cm^{-2}$ enlarged the value of ΔE_p from 154 to 221 mV. Values of the anodic (E_{pa}) and cathodic (E_{pc}) peak potentials estimated at $20\,mV\,s^{-1}$ from Fig. 3 were 535 and 314, 538 and 344, and 500 and 338 mV for A, B and C electrodes, respectively. Recently, a pair of oxidation and reduction peaks prior to the current peak for oxygen evolution have also been reported for a sprayed (s) and layered (l) film of $LaNiO_3$ on Pt ($E^\circ \sim 460$ (s), ~ 470 (l) mV) [4] and a layered film on Ni ($E^\circ \sim 450$ mV) [8]. Comparison of E_{pa} and E_{pc} values obtained in the present investigation with those reported in the literature indicate that the redox couple, Ni^{3+}/Ni^{2+} is formed on the $LaNi_{1-x}Fe_xO_3$ surface during anodic potential cycling conditions.

It was observed that increase in the potential scan rate increased the peak separation potential (ΔE_p) considerably. The ΔE_p value became more than double with a ten fold increase in scan rate. The voltammetric charge (q) was found to vary linearly with the inverse of the square root of scan rate (Fig. 4), showing that the redox processes are diffusion controlled. The charge (q) was determined by integrating

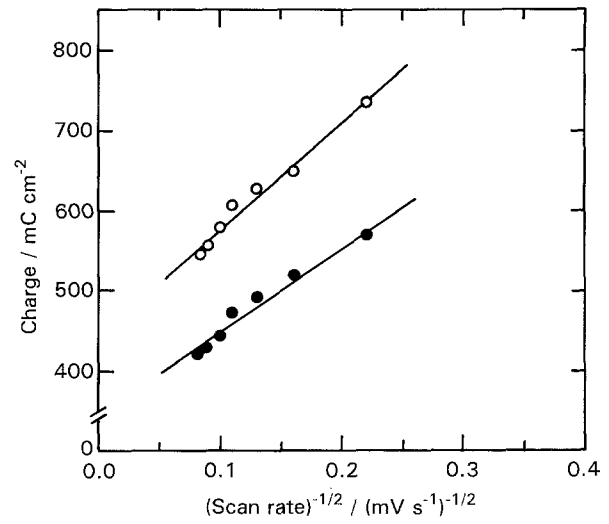

Fig. 4. Plot of charge (q) against (scan rate)$^{-1/2}$. Key: (○) $LaNiO_3$; (●) $LaNi_{0.75}Fe_{0.25}O_3$.

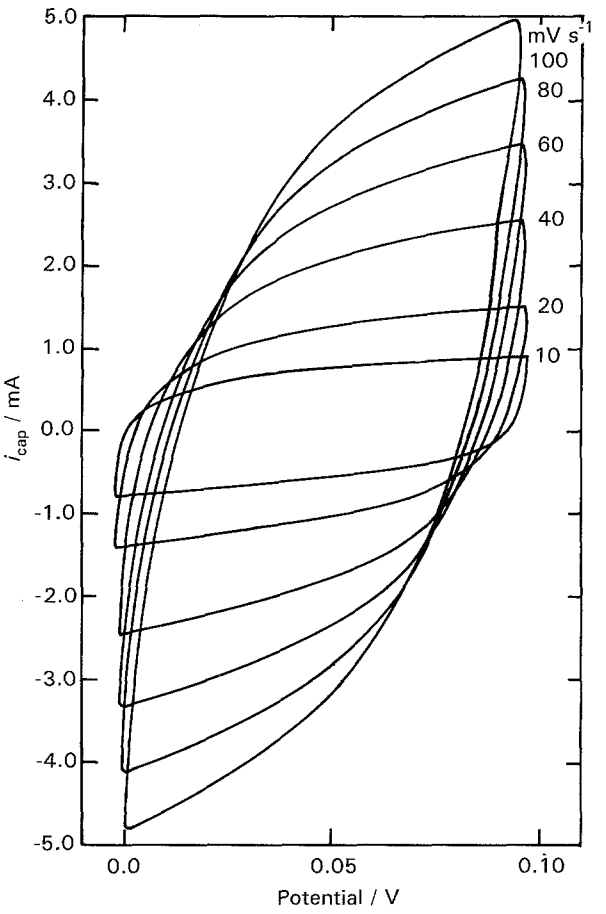

Fig. 5. Cyclic voltammograms of the $LaNiO_3$ electrode (method I), in the potential range 0.0–0.10 V at various scan rates in 1 M KOH (25 °C).

the cyclic voltammetric (CV) curve from zero potential to a potential just prior to the commencement of oxygen evolution.

3.4. *Roughness factor*

To determine the electrochemically active area, cyclic voltammograms of the oxide electrodes were recorded in two different potential regions, 0–100 mV and 50–150 mV at varying scan rates in 1 M KOH. Typical voltammograms for the electrode (A) are shown in Fig. 5. At each scan rate the anodic and cathodic current densities were almost equal in magnitude. As mentioned earlier [4], the charging current density (i_{cap}) was estimated at the middle of the scan range and then plotted as a function of scan rate (Fig. 6). These plots were found to be linear (passing through the origin), particularly at lower scan rates. The double layer capacitance (C_{dl}) value was determined from the slope of the linear part of the curve. The observed deviation from linearity in the case of the oxide obtained by method I indicates that some of the internal oxide surface, particularly microboundaries along the pore walls and the intercrystalline gaps, becomes excluded from the electrolyte contact at higher scan rates [9]. The roughness factor (R) was computed as described earlier [4], by assuming a double layer capacitance of $60\,\mu F\,cm^{-2}$ for smooth oxide surfaces. The

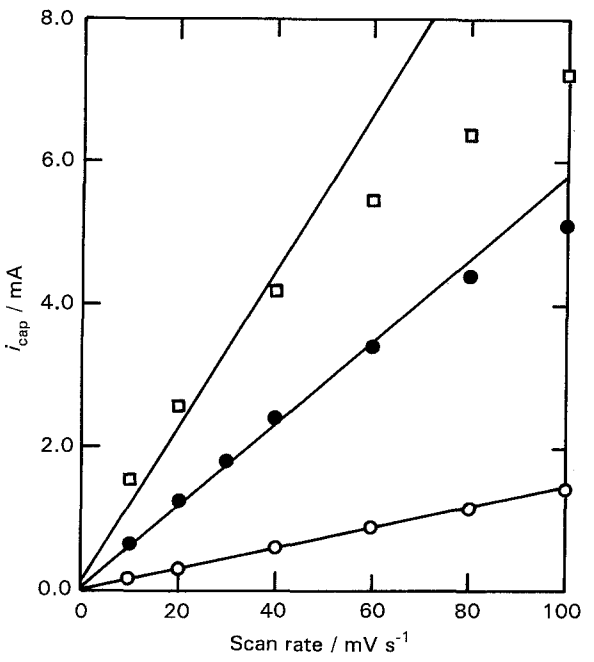

Fig. 6. Plot of capacity current against scan rate in 1 M KOH (25 °C); (□) $LaNiO_3$ and (●) $LaNi_{0.75}Fe_{0.25}O_3$ (method I) and (○) $LaNiO_3$ (method II).

calculated values of roughness factor for different electrodes are shown in Table 1.

The observation of Table 1 shows that the roughness factor for the oxide prepared by method I ($R = 1820$) is about seven times greater than that prepared by method II ($R = 250$). This clearly demonstrates the influence of preparation method on the oxide roughness. Further, the partial substitution of nickel by iron in the oxide resulted in a decrease in roughness factor, the effect being greater with a higher amount of iron substitution. The effect of oxide loading on roughness factor has also been studied and the results are shown in Fig. 7 for electrode A. The roughness factor increased with increase in oxide loading at the beginning and finally attained a constant value. The constancy in R values at higher loading might result from the saturation of the Perovskite crystallites in contact with the electrolyte [8, 9].

3.5. *Tafel plots*

The iR-free E against $\log i$ plots for oxygen evolution at the lanthanum nickelate electrodes were recorded at 0.2 mV s^{-1} in 1 M KOH at 25 °C. Each polarization curve was observed to have a similar form. Their Tafel slope (b) values ranged between 60 and 86 mV decade^{-1} at low current density ($i < 100$ mA cm^{-2}) (Table 1).

To determine the reaction order (p) with respect to OH^- concentration, the oxygen evolution study was carried out at varying KOH concentrations (0.1–1 M) and at constant ionic strength ($\mu = 1.5$). The value of p was estimated from the slope of the log i against log[OH^-] plot at a constant potential across the oxide/KOH interface and was found to be 1.2–1.3 for all the oxide electrodes prepared *in situ*. The representative plots with two active electrodes: $LaNiO_3$ (A) and $LaNi_{0.75}Fe_{0.25}O_3$ (B) are shown in Fig. 8.

Table 1 shows that the apparent electrocatalytic activity of $LaNiO_3$ ($l = 25$ mg cm^{-2}) prepared at 550 and 600 °C by method I is approximately the same but is lower when the oxide is prepared at a higher temperature (700 °C). The observed low apparent electrocatalytic activity can be ascribed to the decrease in roughness. Further, the apparent electrocatalytic activity is highest with an oxide loading of 25–30 mg cm^{-2}. Iron substitution of 0.25 mole was found to enhance greatly, the apparent electrocatalytic activity of the oxide; however, higher substitution had an adverse effect. Thus, based on the values of the overpotential at 100 mA cm^{-2} in 1 M KOH (Table 1) the $Ni/LaNi_{0.75}Fe_{0.25}O_3$ electrode, B, ($\eta_{O_2} = 395$ mV) was found to be most active. This had ~ 30 mV lower overpotential than electrode A ($\eta_{O_2} = 428$ mV). It is noteworthy that the electrode C, which has been reported as one of the best anodes in the form of pellets [1], showed the lowest activity ($\eta_{O_2} = 476$ mV) in the form of film. The observed difference in apparent electrocatalytic activity of electrodes A ($\eta_{O_2} = 428$ mV at 100 mA cm^{-2}) and C ($\eta_{O_2} = 476$ mV at 100 mA cm^{-2}) can be ascribed to the variation in the oxide roughness factor (Table 1). The low activity of the electrode C can

Table 1. Values of the electrode kinetic parameters for oxygen evolution on lanthanum nickelate in 1 M KOH solution at 25 °C

Electrodes	*Preparation temperature* /°C	*Oxide loading* /mg cm^{-2}	*Resistance* /Ω	*R*	*b* /mV dec^{-1}	η_{O_2}/mV *at* i/mA cm^{-2} *10*	*100*
$LaNiO_3$	600	4.4	0.9	248	68	378	515
$LaNiO_3$	600	8.8	1.2	468	68	329	465
$LaNiO_3$	600	11.7	1.1	1092	70	329	455
$LaNiO_3$ (A)	600	25.4	0.8	1820	73	315	428
$LaNiO_3$	600	29.6	1.2	1616	86	303	432
$LaNiO_3$	550	25.7	1.2	1417	66	321	438
$LaNiO_3$	700	25.2	0.9	149	60	353	485
$LaNi_{0.75}Fe_{0.25}O_3$ (B)	600	26.1	1.0	1041	62	323	395
$LaNi_{0.5}Fe_{0.5}O_3$	600	26.0	1.3	484	59	338	437
$LaNiO_3$ (C)	800	22.4	0.9	246	67	360	476

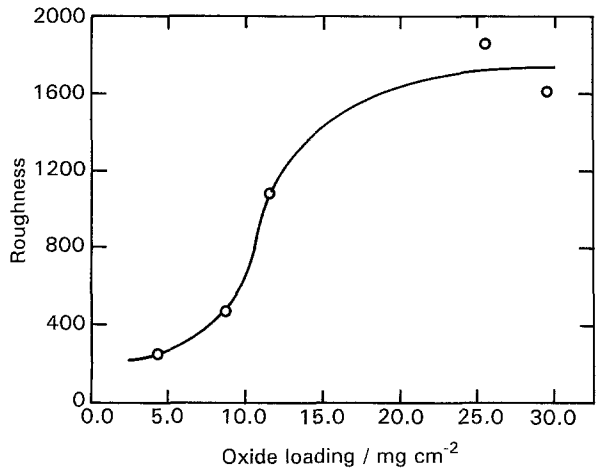

Fig. 7. The effect of oxide loading on the roughness factor in the case of $LaNiO_3$ electrode prepared by method I.

also be related to the impurities in the oxide (Fig. 1).

The oxygen evolution reaction on $LaNiO_3$ has also been studied by other workers. Depending on the method of preparation, and other experimental conditions, varying values of the Tafel slope and the reaction order were found. Bockris and Otagawa [10] observed a Tafel slope of 65–130 mV decade^{-1} on $LaNiO_3$ prepared by the ceramic method while they found a single Tafel slope of 43 mV decade^{-1} up to a current density of 100 mA cm^{-2} on the same oxide prepared by the coprecipitation technique [1]. Singh *et al.* [4] also observed a single Tafel slope of 40 mV decade^{-1} on the sprayed $LaNiO_3$ film on Pt where as on a layer film of $LaNiO_3$ they found 65 mV decade^{-1}.

As observed in this study, the first order oxygen evolution reaction with respect to OH^- concentration has also been reported elsewhere [4, 8, 10]. The reaction order and the Tafel slope observed with the catalytic films prepared *in situ* indicate a mechanism similar to that proposed in [10].

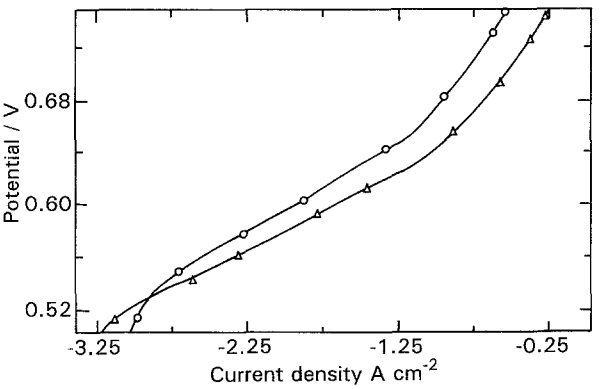

Fig. 9. Tafel plots for oxygen evolution on the active catalytic films in 30 wt % KOH (25° C); (○) $LaNiO_3$ and (△) $LaNi_{0.75}Fe_{0.25}O_3$ (method I).

The oxygen evolution reaction on active electrodes was also studied in commercial KOH solution (30 wt %) at 25 °C (Fig. 9). The results showed that at 500 mA cm^{-2}, the $LaNi_{0.75}Fe_{0.25}O_3$ electrode (B) had ~ 86 mV lower oxygen overpotential than $LaNiO_3$ (A). Thus, the performance of the electrode B is superior even at practical current densities in 30 wt % KOH.

The stability of $LaNiO_3$ film obtained by both preparation methods was also examined at a current density of 100 mA cm^{-2} in 30 wt % KOH at 25 °C. The study indicated a reasonably stable potential for over 48 h of investigation (Fig. 10).

4. Conclusion

The study indicates that the hydroxide solid solution precursor method is economical compared to the hydroxide coprecipitation method. The catalyst prepared by the former method was found to be electrocatalytically more active. 0.25 mole iron-substitution for nickel in the oxide lattice reduced the oxygen overpotential by over 80 mV at 500 mA cm^{-2} in 30 % KOH at 25 °C.

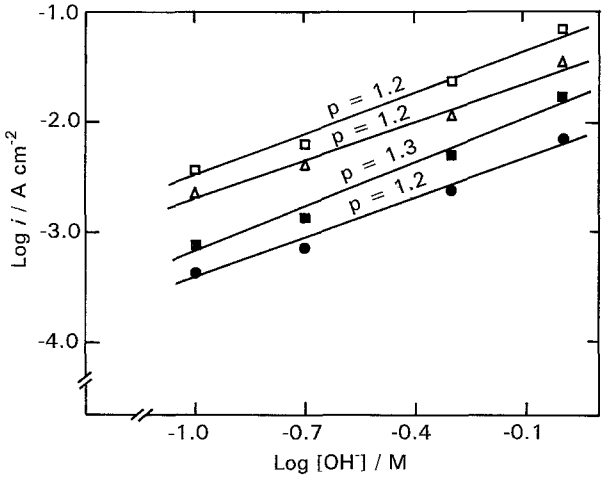

Fig. 8. Plot of log i against log [OH^-] at different potential across the oxide/KOH solution interface (25 °C). $LaNiO_3$: (●) 0.65 V and (■) 0.67 V; $LaNi_{0.75}Fe_{0.25}O_3$: (△) 0.67 V and (□) 0.69 V.

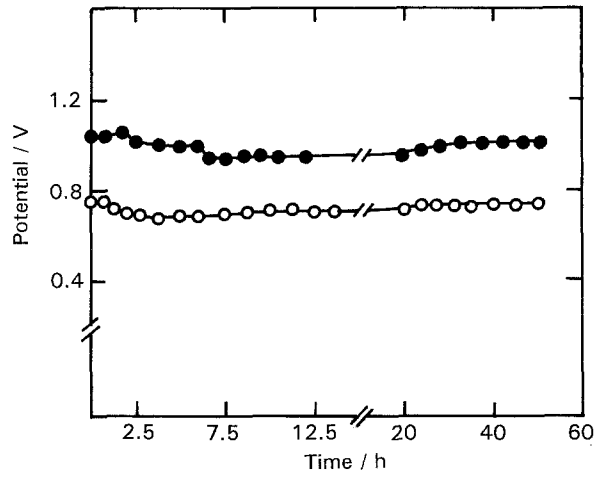

Fig. 10. Performance of the $LaNiO_3$ electrode prepared by two different methods in 30 wt % KOH (25 °C); (○) $LaNiO_3$ (method I) and (●) $LaNiO_3$ (method II). i = 100 mA cm^{-2} (without iR correction).

Acknowledgement

Financial support from the Indo-French Centre for the Promotion of Advanced Research (Centre Franco-Indien pour la Promotion de la Recherche Avancee), New Delhi, India, is gratefully acknowledged.

References

[1] T. Otagawa and J. O'M. Bockris, *J. Electrochem. Soc.* **129** (1982) 2391.
[2] K. Vidyasagar, J. Gopalakrishnan and C. N. R. Rao, *J. Solid State Chem.* **58** (1985) 29.
[3] A. Daghetti, G. Lodi and S. Trasatti, *Mater. Chem. Phys.* **8** (1983) 1.
[4] R. N. Singh, Lal Bahadur, J. P. Pandey, S. P. Singh, P. Chartier and G. Poillerat, *J. Appl. Electrochem.* **24** (1994) 149.
[5] S. K. Tiwari, P. Chartier and R. N. Singh, *J. Electrochem. Soc.* **142** (1995) 148.
[6] R. N. Singh, J. K. Koenig, G. Poillerat and P. Chartier, *ibid.* **137** (1990) 1408.
[7] A. K. Ladavos and P. J. Pomonis, *J. Chem. Soc. Faraday Trans.* **87** (1991) 3291.
[8] S. P. Singh, R. N. Singh, G. Poillerat and P. Chartier, *Int. J. Hydrogen Energy* **20** (1994) 203.
[9] R. Boggio, A. Carugati and S. Trasatti, *J. Appl. Electrochem.* **17** (1987) 828.
[10] J. O'M. Bockris and T. Otagawa, *J. Phys. Chem* **87** (1983) 2960.